Arab J Geosci (2016) 9: 42
DOI 10.1007/s12517-015-2089-8

ORIGINAL PAPER

Hydrogeochemical processes constrained by multivariate statistical methods and isotopic evidence of groundwater recharge in the aquifer of Figuig, Eastern High Atlas of Morocco

Abdelhakim Jilali[1] · **Nathalie Fagel**[2] · **Mounir Amar**[3] · **Mahmoud Abbas**[4] · **Yassine Zarhloule**[1]

Received: 1 September 2014 / Accepted: 10 September 2015 / Published online: 11 December 2015

Abstract In this paper, we present and discuss 72 samples of groundwater (borehole, well, and spring), collected over a period of time of 20 years (i.e., between 1983 and 2004) in the Figuig aquifer. The chemical and isotopic analyses were carried out to improve our understanding of the hydrogeochemical processes. Most of the waters sampled consist of Ca-Mg-HCO_3 and Na-K-Cl types. The samples are grouped according to two factors. Factor 1 shows strong negative loadings of EC, Cl-, Na^+, Ca^{2+}, Mg^{2+}, and NO^{3-}, K^+ with 73.91 % of the total variance (TV); factor 2 shows strong positive loadings of SO_4^{2-}, HCO^{3-} with TV of 11.02 %. The ^{18}O and ^{2}H values of well and spring waters are linearly correlated, in a similar manner to the World Meteoric Water Line (WMWL). The ^{14}C datings indicate that the age of groundwater obtained using different models ranges between 2495 and 10,696 years.

Keywords Hydrogeochemistry · Statistical analysis · Isotopes · Figuig aquifer · Morocco

✉ Abdelhakim Jilali
yamaapa@hotmail.com

[1] Laboratory of Mineral Deposits, Hydrogeology & Environment, Faculty of Sciences, University Mohammed I, Boulevard Mohammed VI, BP: 524, 60000 Oujda, Morocco

[2] Department of Geology, Faculty of Science, University of Liege, Liege, Belgium

[3] Department of Geology, Faculty of Science, University of Moulay Ismail Meknes, Meknes, Morocco

[4] Laboratory of Water Analysis of Figuig (L.A.E.F), Municipality of Figuig, BP 121, Administrative Centre, 61000 Figuig, Morocco

Introduction

Water resources are under serious pressure worldwide, and their efficient management and protection constitute a key issue for the future (Wildemeersch et al. 2010). This plays a vital role in the socioeconomic development in arid and semi-arid regions (Tlili-Zrelli et al. 2013). Understanding the local hydrogeological system helps manage and protect groundwater resources (Wildemeersch et al. 2010). The chemical composition of groundwaters depends on the available precipitation, bedrock geology, and various geochemical processes, and their concentrations vary with residence time. Numerous studies were carried out to evaluate the impact of hydrogeochemical processes on water resources as this is a frequent objective of hydrogeological research (Abderamane et al. 2013; Kumar et al. 2013; Thivya et al. 2013; Tlili-Zrelli et al. 2013; Wang et al. 2013; Wildemeersch et al. 2010; Wu et al. 2013; Zhai et al. 2013).

A very suitable natural laboratory to study these processes is the Figuig Basin in Eastern Morocco, where the deterioration of groundwater quantity and quality is significant. This deterioration is evidenced by the decrease in the water output of springs, the increase of water salinity, and the contamination by wastewaters (Jilali 2014a, b; Jilali et al. 2015a). For this reason, geological and hydrogeological research in the Figuig region has been the focus of the studies of Jilali et al. (2015b) and Jilali and Zarhloule (2015). The main objective of the present work is to improve the understanding of hydrogeochemical processes in this region. To achieve this objective, we used stable isotopes (D and ^{18}O), radioactive isotopes (^{3}H and ^{14}C), and major ion chemistry (K^+, Na^+, Ca^{2+}, Mg^{2+}, HCO_3^-, Cl^-, SO_4^{2-}, NO_3^-). We have applied various graphical representations and maps to classify and interpret the geochemical data we have obtained.

Study area

The Figuig Region study area is located near the Morocco-Algeria border, in the Eastern High Atlas of Morocco, and is bound by several mountains (Jbels Grouz, el Haïmeur, Mélias, Zenaga Tarhla, and Sidi Youssef). The most important wadi (river) is Zouzfana located to the east of the Figuig Oasis. It lies between latitude 32° 4′ N and 32° 9′ N and longitude 1° 20′ and 1° 10′ W, and covers an area of about 60 km^2 (Fig. 1). The climate of the region is arid, with average rainfall of about 120 mm/year (Jilali 2014a, b; Jilali and Zarhloule 2015; Jilali et al. 2015c).

Geological and hydrogeological background

The geology of the region is formed by Mesozoic and Cenozoic formations. The principal Mesozoic sedimentation occurred in the Triassic and Jurassic (Lias and Dogger). The Cretaceous (InfraCenomanian) is only present on the Algerian side of the Morocco-Algeria border, and the region is covered by Quaternary formations. The stratigraphic sequence consists of (1) red-green clays and basaltic tuffs of Triassic age, (2) Hettengian-Pliensbachian formations of limestones and dolostones, (3) a Toarcian formation composed of alternating limestones and marls, (4) Aalenian limestone formations, (5) a Bajocian formation composed of alternating limestones and marls, followed by a sequence of limestones, and (6) a Quaternary formation composed of alluviums, sand, and travertine (Jilali 2014a; Jilali et al. 2015b; Jilali and Zarhloule 2015). This area is very much fractured and presents two principal fault systems oriented 70° N and 140° N (Fig. 2). A more detailed geological description can be found in Jilali (2014a). Jilali et al. (2015b). and Jilali and Zarhloule (2015).

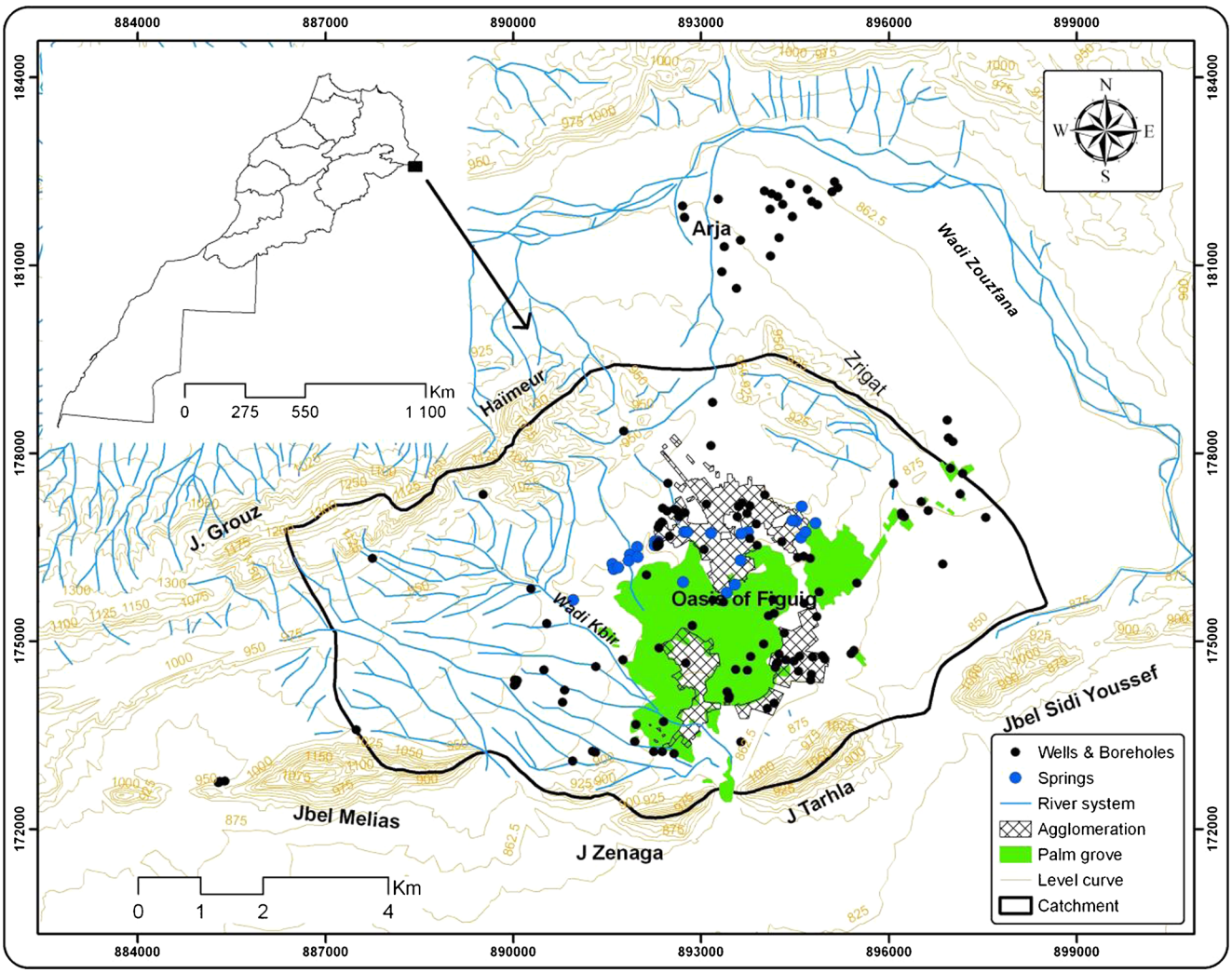

Fig. 1 Location of the study area

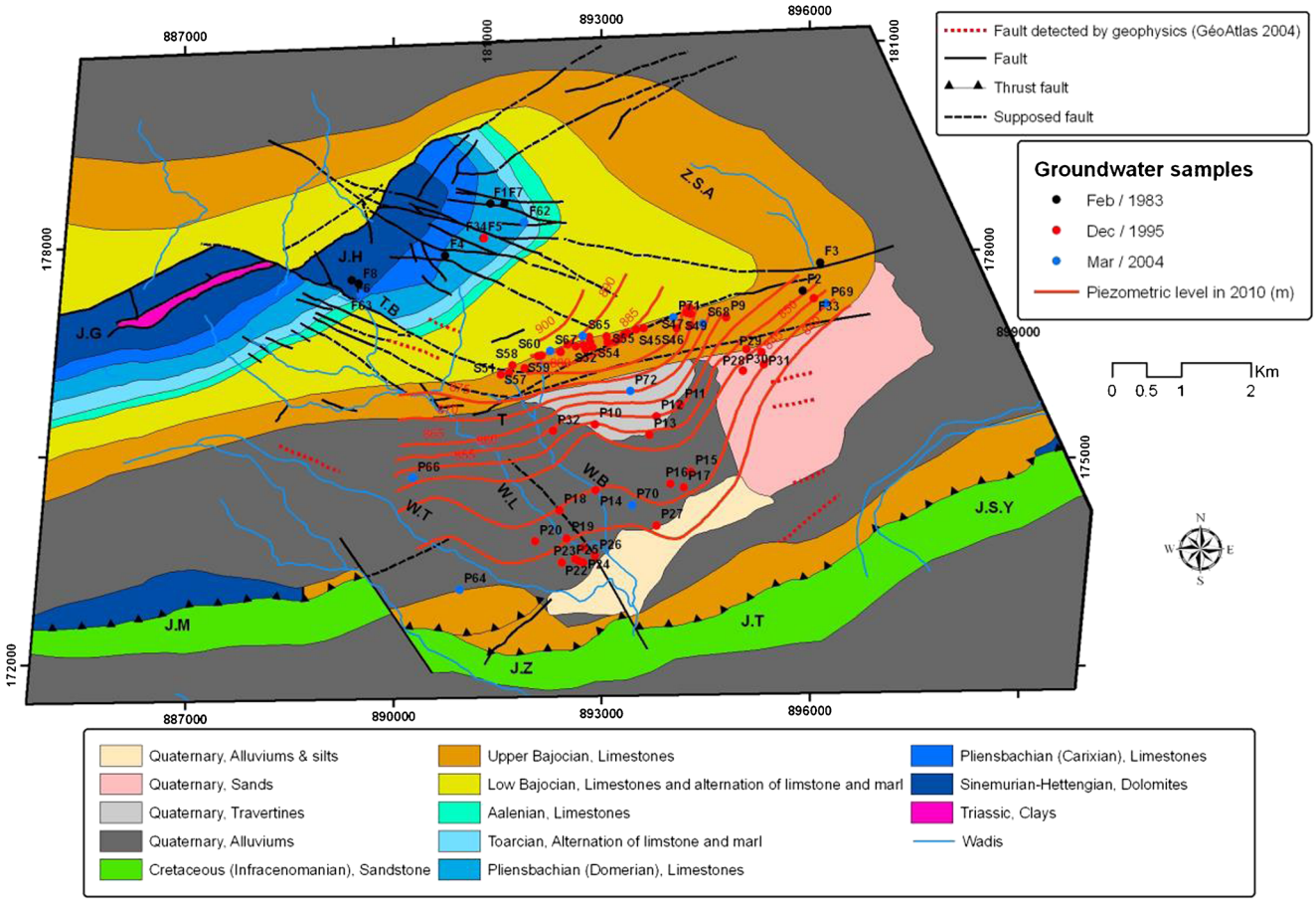

Fig 2 Geological and hydrogeological map of the study area and groundwater samples. *J.G* Jbel Grouz, *J.H* Jbel el Haïmeur, *Z.S.A* Zrigat Sidi Abdelkader, *T.B* Tiniet el Bida, *T* Tachroumt, *W.B* Wadi Bouchalikane, *W.L* Wadi Lakbir, *W.T* Wadi Tazoukart, *J.M* Jbel Mélias, *J.Z* Jbel Zenaga, *J.T* Jbel Tarhla, *J.S.Y* Jbel Sidi Youssef (Jilali 2014; Jilali et al. 2015; Jilali and Zarhloule 2015). modified

The Figuig Region is a good example of an unconfined multilayer aquifer (Jilali 2014a; Jilali and Zarhloule 2015). It is exploited by wells, boreholes, and springs, essentially in the Quaternary and Dogger layers. The Lias aquifer is exploited on the mountain of el Haïmeur by two boreholes providing table water supply and by another borehole in Tiniet el Bida, where the water is used for irrigation. The water flow has two main directions: from north to south and from north-west to south-east (Fig. 2). The groundwater level is at a depth of between 10 and 20 m in the south and 40–60 m in the west and north (Jilali 2014a, b; Jilali et al. 2015b; Jilali and Zarhloule 2015).

Methodology

Sample collection and analysis

A total of 72 groundwater samples (F: borehole; P: well and S: spring) were collected from the study area (Table 1). The electric conductivity (EC), major ion chemistry (K^+, Na^+, Ca^{2+}, Mg^{2+}, HCO_3^-, Cl^-, SO_4^{2-}, NO_3^-), ^2H, ^{18}O, ^3H, ^{14}C, and ^{13}C analyses (vintage 1983 and 2004) were done by the Hydraulic Basin Agency of Moulouya (HBAM) except for the 1995 vintage data, which were done by Assou (1996). The methods of analysis used for the major ions were SKALAR and Rodier (1984). whereas the isotope analysis was performed in the CNESTEN (National Center of Energy Sciences and Nuclear Techniques of Morocco). The precision of the chemical analyses was defined by checking ionic charge balance. The acceptable error on the ion balance is taken at a maximum of 10 %.

Statistical analysis & geochemical modeling

The Principal Component Analysis (PCA) multivariate statistical technique was used in our research. This method is a quantitative and independent approach for the classification of groundwater samples according to their geochemical

Table 1 Electrical conductivity (EC in μS/Cm), concentrations of the main chemical species (in mg/l) and isotopic geochemistry of groundwater samples collected

Name	Year	EC (μS/cm)	Ca^{2+} (mg/l)	Mg^{2+} (mg/l)	Na^{+} (mg/l)	K^{+} (mg/l)	HCO_3^{-} (mg/l)	Cl^{-} (mg/l)	$SO^{4-}{}_2$ (mg/l)	NO_3^{-} (mg/l)	$\delta^{18}O$ (‰)	$\delta^{2}H$ (‰)	^{3}H (TU)	^{14}C (pCm)	^{13}C (‰)
F1	Feb 1983	2130	78	44.77	380	8.1	262.3	560.9	201.6	9	–	–	–	–	–
F2	Feb 1983	3820	150	82.28	620	9.8	280.6	997.5	297.6	43	–	–	–	–	–
F3	Feb 1983	2050	50	33.88	370	9	273.9	461.5	230.4	14	–	–	–	–	–
F4	Feb 1983	2260	86	38.72	400	8.8	262.3	564.45	206.4	12	–	–	–	–	–
F5	Feb 1983	2010	80	42.35	390	7.7	268.4	553.8	192	14	–	–	–	–	–
F6	Feb 1983	2250	76	41.14	400	7.3	250.1	571.55	196.8	15	–	–	–	–	–
F7	Feb 1983	2280	86	47.19	360	7.8	317.2	560.9	129.6	6	–	–	–	–	–
F8	Feb 1983	2280	88	43.56	300	7.8	305	582.2	33.6	14	–	–	–	–	–
P9	Dec 1995	3010	140	36.3	448.04	7.82	427	745.5	69.6	13.64	–	–	–	–	–
P10	Dec 1995	5190	160	72.6	985.55	19.55	610	1313.5	480	21.08	–	–	–	–	–
P11	Dec 1995	4400	142.6	53.24	824.55	39.1	549	1153.75	295.2	45.26	–	–	–	–	–
P12	Dec 1995	4620	140	65.34	840.65	19.55	610	1331.25	302.4	34.72	–	–	–	–	–
P13	Dec 1995	6270	182	67.76	1216.7	39.1	610	1686.25	513.6	24.8	–	–	–	–	–
P14	Dec 1995	8180	300	181.5	1173	35.19	793	2041.25	502.56	57.66	–	–	–	–	–
P15	Dec 1995	6000	280	169.4	690	19.55	488	1686.25	109.92	44.02	–	–	–	–	–
P16	Dec 1995	11580	500	314.6	1449	31.28	671	3372.5	469.92	62.62	–	–	–	–	–
P17	Dec 1995	6530	200	284.35	786.6	39.1	488	1952.5	296.16	57.66	–	–	–	–	–
P18	Dec 1995	7080	276	323.07	821.1	15.64	488	1952.5	563.52	53.32	–	–	–	–	–
P19	Dec 1995	12270	620	314.6	1437.5	58.65	488	3976	9.6	93	–	–	–	–	–
P20	Dec 1995	2270	180	12.1	437.46	8.99	366	621.25	101.28	39.68	–	–	–	–	–
P21	Dec 1995	13100	524	544.5	1403	19.55	488	4082.5	459.36	70.06	–	–	–	–	–
P22	Dec 1995	5010	180	39.33	438.84	10.95	366	710	245.28	31	–	–	–	–	–
P23	Dec 1995	1530	160	27.23	196.42	5.47	366	355	96	37.82	–	–	–	–	–
P24	Dec 1995	5000	360	84.7	655.5	19.55	427	1597.5	48	50.22	–	–	–	–	–
P25	Dec 1995	3500	180	60.5	460	29.33	427	887.5	96	34.72	–	–	–	–	–
P26	Dec 1995	6350	360	96.8	747.5	19.55	488	1775	192	56.42	–	–	–	–	–
P27	Dec 1995	8890	200	145.2	1377.7	39.1	305	2516.95	372.96	60.76	–	–	–	–	–
P28	Dec 1995	6900	200	75.63	1182.2	19.55	610	1739.5	408.48	39.68	–	–	–	–	–
P29	Dec 1995	5690	140	78.65	1049.95	19.55	488	1526.5	381.12	44.02	–	–	–	–	–
P30	Dec 1995	5730	168	79.86	1099.4	39.1	671	1491	460.8	34.1	–	–	–	–	–
P31	Dec 1995	5970	178	85.91	1132.75	39.1	549	1597.5	552.96	45.26	–	–	–	–	–
P32	Dec 1995	7630	156	87.12	1386.9	39.1	854	2041.25	215.52	19.22	–	–	–	–	–
F33	Dec 1995	1950	64.13	21.4	370	8	366	488.11	74.25	0.42	–	–	–	–	–
F34	Dec 1995	1860	102.6	31.13	284	6.8	260.4	503.74	66.73	1.23	–	–	–	–	–
S35	Dec 1995	2230	120	24.2	329.82	7.82	305	532.5	108.96	16.74	–	–	–	–	–
S36	Dec 1995	2200	100	48.4	314.18	7.82	366	497	126.72	13.64	–	–	–	–	–
S37	Dec 1995	2210	80	36.3	324.3	15.64	366	532.5	10.08	17.98	–	–	–	–	–
S38	Dec 1995	2130	137	62.92	226.55	5.87	366	532.5	24.96	14.26	–	–	–	–	–
S39	Dec 1995	2200	100	60.5	316.94	7.82	366	532.5	108	14.26	–	–	–	–	–
S40	Dec 1995	2240	80	48.4	322	7.82	366	532.5	46.56	16.74	–	–	–	–	–
S41	Dec 1995	2240	120	48.4	321.54	7.82	366	532.5	134.88	16.74	–	–	–	–	–
S42	Dec 1995	2350	100	60.5	338.1	15.64	366	532.5	179.04	22.94	–	–	–	–	–
S43	Dec 1995	2370	100	72.6	339.02	7.82	366	532.5	220.32	21.7	–	–	–	–	–
S44	Dec 1995	2410	120	48.4	340.86	7.82	427	568	74.4	29.14	–	–	–	–	–
S45	Dec 1995	2430	120	36.3	315.1	7.82	366	532.5	68.64	29.14	–	–	–	–	–
S46	Dec 1995	2470	100	48.4	349.14	15.64	366	568	105.6	23.56	–	–	–	–	–
S47	Dec 1995	2370	100	48.4	342.24	7.82	366	621.25	14.88	15.5	–	–	–	–	–

Table 1 (continued)

Name	Year	EC (μS/cm)	Ca^{2+} (mg/l)	Mg^{2+} (mg/l)	Na^{+} (mg/l)	K^{+} (mg/l)	HCO_3^{-} (mg/l)	Cl^{-} (mg/l)	$SO^{4-}{}_2$ (mg/l)	NO_3^{-} (mg/l)	$\delta^{18}O$ (‰)	$\delta^{2}H$ (‰)	^{3}H (TU)	^{14}C (pCm)	^{13}C (‰)
S48	Dec 1995	2390	100	48.4	324.3	7.82	305	568	49.92	16.12	–	–	–	–	–
S49	Dec 1995	2380	100	48.4	340.86	7.82	366	603.5	32.16	15.5	–	–	–	–	–
S50	Dec 1995	2510	120	36.3	345.92	7.82	366	621.25	7.2	17.98	–	–	–	–	–
S51	Dec 1995	1560	60	36.3	243.8	7.82	305	355	67.2	19.22	–	–	–	–	–
S52	Dec 1995	2230	100	60.5	322	15.64	366	532.5	153.12	13.02	–	–	–	–	–
S53	Dec 1995	2200	100	48.4	289.34	7.82	366	532.5	25.92	14.88	–	–	–	–	–
S54	Dec 1995	2530	100	60.5	376.05	23.46	427	621.25	109.44	12.4	–	–	–	–	–
S55	Dec 1995	2240	100	27.23	354.2	19.55	366	532.5	136.8	18.6	–	–	–	–	–
S56	Dec 1995	2600	80	9.08	492.2	7.82	366	621.25	125.76	14.26	–	–	–	–	–
S57	Dec 1995	3130	100	60.5	530.84	9.78	366	887.5	99.84	15.5	–	–	–	–	–
S58	Dec 1995	3160	100	84.7	496.8	7.82	427	798.75	193.44	16.74	–	–	–	–	–
S59	Dec 1995	3390	80	72.6	552.23	9.78	366	887.5	152.16	11.16	–	–	–	–	–
S60	Dec 1995	2890	120	60.5	346.15	15.64	366	621.25	125.76	21.08	–	–	–	–	–
S61	Dec 1995	2400	120	48.4	349.6	15.64	366	621.25	84.96	20.46	–	–	–	–	–
F62	Mar 2004	2060	96.7	31.1	282	8.23	305	453.16	72.9	14.56	−9.01	−60.03	1.2	22.31	−7.63
F63	Mar 2004	2090	88	30.72	273	7.13	305	447.77	73.7	16.55	−9.12	−60.04	0.4	22.36	−7.93
P64	Mar 2004	900	44.4	37.4	81	6.22	305	96.61	133.8	13.19	−8.3	−56.16	1.7	–	–
S65	Mar 2004	2100	83.9	30.95	284	8.43	292.8	450.67	77.8	15.8	−8.95	−60.61	1.4	–	–
P66	Mar 2004	460	42.8	14.97	31	1.21	274.5	12.06	28	19.6	−8.71	−57.65	0.9	33.76	−7.4
S67	Mar 2004	2410	78.5	31.07	287	8.63	292.8	468.31	77.8	16.57	−9.11	−61.91	1.2	–	–
S68	Mar 2004	2330	93.4	33.02	292	8.51	280.6	497.98	79.6	20.78	−9.07	−59.5	0.3	–	–
P69	Mar 2004	2470	101.8	47.75	375	8.73	323.3	580.64	136.7	30.95	−8.42	−54.88	2.9	–	–
P70	Mar 2004	5600	200.1	103.59	847	16.54	597.8	1810.37	312.2	69.25	−8.34	−61.33	1	–	–
P71	Mar 2004	2940	131	49.53	319	8.68	274.5	609.44	117.4	46.96	−9.05	−62.12	0.9	32.03	−8.07
P72	Mar 2004	2880	117.9	40.2	277	12.33	427	358.83	100.2	53.95	−9.01	−59.94	0.6	–	–

From HBAM (1983, 2004) and Assou 1996, 1995

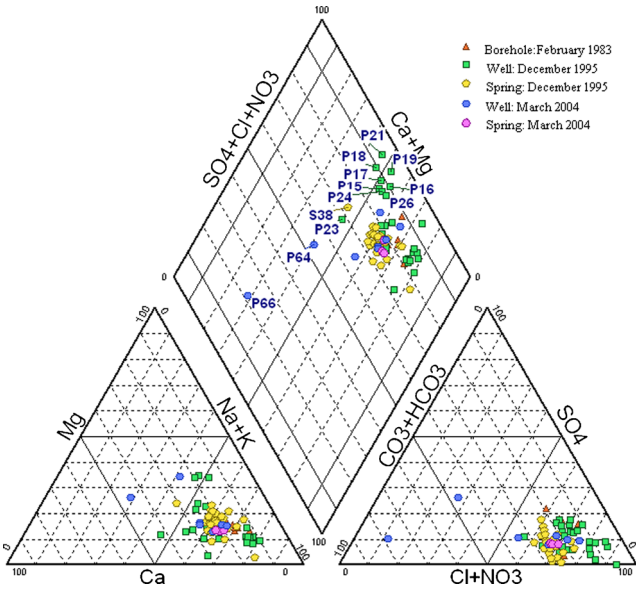

Fig. 3 Piper diagram for the major ions for different years

Table 2 Water type

Samples	Water type
F34, F62, F63, F8, P20, P23, P25, P69, P72, P9, S35, S36, S41, S44-S50, S53, S55, S60, S61, S65, S67, and S68	Na-Ca-Cl-HCO_3
F1, F2, F4-F6, P10-P14, P27-P32, P70, S57, and S59	Na-Cl
F33, F7, S37, S40, S42, S51, S54, and S56	Na-Cl-HCO_3
P22, P24, P26, and P71	Na-Ca-Cl
S38, S39, and S52	Na-Ca-Mg-Cl-HCO_3
P64	Na-Mg-Ca-HCO_3-SO_4-Cl
P17, P18, and P21	Na-Mg-Cl
P15 and P19	Na-Ca-Mg-Cl
S43 and S58	Na-Mg-Cl-HCO_3
P66	Ca-Na-Mg-HCO_3
F3	Na-Cl-SO4-HCO_3
P16	Na-Mg-Ca-Cl

Table 3 Saturation indices of Figuig groundwater

Name	SI (anhydrite)	SI (aragonite)	SI (calcite)	SI (dolomite)	SI (gypsum)
F1	−1.71	−0.47	−0.32	−0.54	−1.49
F2	−1.41	−0.23	−0.09	−0.08	−1.19
F3	−1.82	−0.63	−0.49	−0.8	−1.6
F4	−1.66	−0.43	−0.28	−0.56	−1.44
F5	−1.72	−0.44	−0.3	−0.53	−1.5
F6	−1.73	−0.5	−0.35	−0.62	−1.51
F7	−1.86	−0.33	−0.18	−0.28	−1.64
F8	−2.4	−0.31	−0.16	−0.28	−2.18
P9	−1.96	−0.01	0.14	0.04	−1.74
P10	−1.26	0.07	0.21	0.43	−1.04
P11	−1.45	0.02	0.16	0.24	−1.24
P12	−1.47	0.04	0.19	0.39	−1.25
P13	−1.22	0.1	0.24	0.41	−1
P14	−1.11	0.39	0.54	1.22	−0.89
P15	−1.71	0.23	0.38	0.9	−1.49
P16	−1.05	0.49	0.63	1.43	−0.83
P17	−1.49	0.05	0.19	0.89	−1.27
P18	−1.12	0.15	0.29	1.01	−0.91
P19	−2.65	0.46	0.6	1.28	−2.44
P20	−1.68	0.04	0.18	−0.46	−1.46
P21	−1.12	0.34	0.48	1.35	−0.9
P22	−1.35	0	0.14	−0.03	−1.13
P23	−1.7	0.02	0.17	−0.08	−1.48
P24	−1.92	0.31	0.45	0.63	−1.7
P25	−1.77	0.07	0.22	0.31	−1.55
P26	−1.35	0.33	0.48	0.74	−1.13
P27	−1.37	−0.17	−0.02	0.17	−1.15
P28	−1.27	0.15	0.29	0.52	−1.05
P29	−1.41	−0.08	0.07	0.24	−1.19
P30	−1.28	0.12	0.26	0.55	−1.06
P31	−1.19	0.05	0.19	0.41	−0.98
P32	−1.67	0.19	0.33	0.77	−1.45
F33	−2.16	−0.37	−0.22	−0.57	−1.94
F34	−2.02	−0.3	−0.16	−0.49	−1.8
S35	−1.77	−0.19	−0.05	−0.44	−1.55
S36	−1.8	−0.2	−0.06	−0.08	−1.58
S37	−2.95	−0.26	−0.12	−0.22	−2.73
S38	−2.38	−0.05	0.1	0.21	−2.16
S39	−1.89	−0.2	−0.06	0.02	−1.67
S40	−2.31	−0.28	−0.13	−0.13	−2.09
S41	−1.71	−0.13	0.01	−0.02	−1.49
S42	−1.68	−0.22	−0.08	−0.02	−1.46
S43	−1.61	−0.23	−0.09	0.03	−1.39
S44	−1.97	−0.06	0.09	0.13	−1.75
S45	−1.98	−0.11	0.03	−0.1	−1.76
S46	−1.89	−0.2	−0.06	−0.08	−1.67
S47	−2.72	−0.18	−0.04	−0.04	−2.5

Table 3 (continued)

Name	SI (anhydrite)	SI (aragonite)	SI (calcite)	SI (dolomite)	SI (gypsum)
S48	−2.19	−0.26	−0.12	−0.2	−1.97
S49	−2.39	−0.19	−0.04	−0.05	−2.17
S50	−2.96	−0.1	0.04	−0.08	−2.74
S51	−2.21	−0.45	−0.3	−0.48	−1.99
S52	−1.74	−0.21	−0.07	−0.01	−1.52
S53	−2.47	−0.18	−0.03	−0.02	−2.25
S54	−1.9	−0.15	−0.01	0.12	−1.68
S55	−1.76	−0.2	−0.06	−0.33	−1.54
S56	−1.88	−0.3	−0.16	−0.91	−1.66
S57	−1.97	−0.24	−0.09	−0.05	−1.75
S58	−1.72	−0.19	−0.05	0.19	−1.5
S59	−1.9	−0.34	−0.2	−0.09	−1.68
S60	−1.77	−0.14	0	0.06	−1.55
S61	−1.92	−0.13	0.02	−0.01	−1.7
F62	−2	−0.26	−0.12	−0.38	−1.78
F63	−2.03	−0.3	−0.16	−0.42	−1.81
P64	−1.98	−0.55	−0.41	−0.55	−1.76
S65	−2.03	−0.34	−0.19	−0.47	−1.81
P66	−2.54	−0.53	−0.39	−0.88	−2.32
S67	−2.05	−0.37	−0.22	−0.5	−1.84
S68	−1.99	−0.32	−0.17	−0.45	−1.77
P69	−1.78	−0.26	−0.11	−0.2	−1.56
P70	−1.37	0.16	0.3	0.68	−1.15
P71	−1.74	−0.21	−0.07	−0.21	−1.52
P72	−1.82	−0.05	0.09	0.07	−1.6

characteristics and may simplify and organize large data sets in order to make useful groupings of similar samples (Kumar et al. 2013; Tlili-Zrelli et al. 2013; Wu et al. 2013). The STATISTICA software was used to process the 1995 vintage data analyses. For this, the analyses of EC, K^+, Na^+, Ca^{2+}, Mg^{2+}, HCO_3^-, Cl^-, SO_4^{2-}, and NO_3^- were used as variables. To investigate thermodynamic controls of mineral-water interactions, the geochemical modeling software PHREEQC (Parkhurst and Appelo 1999) was used to calculate the mineral saturation index (SI).

Results and discussion

Groundwater chemistry

According to Table 1, the EC of groundwater ranges from 1530 to 13,100 μS/Cm. It is low in the western and northern part of the study area and high in the southern. Figure 3 and Table 2 show major cations and anions for underlining possible correlations between host rock lithology and the observed hydrogeochemical facies. The majority of groundwater samples as identified using a Piper diagram and the AquaChem software are Na-Ca-Cl-HCO3 (Jurassic carbonates formations) and Na-K-Cl (Quaternary formations) type waters (Table 2). The latter water type is probably related to anthropogenic activities (irrigation and wastewater) taking place in the southern area.

Saturation index

The Saturation Indices (SI) of the minerals calcite, dolomite, gypsum, aragonite, and anhydrite were calculated using the PHREEQC code. The results of the modeling are shown in Table 3. Saturation indices less than zero indicate that the groundwater is undersaturated with respect to that particular mineral, those equal to zero that the groundwater is saturated, whereas a Saturation Index superior to zero indicates a

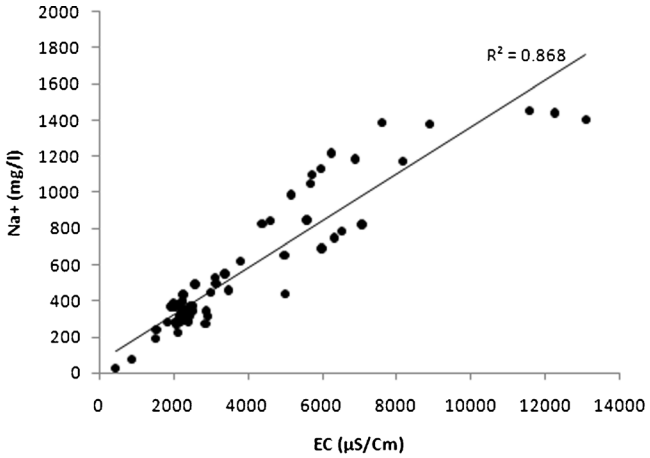

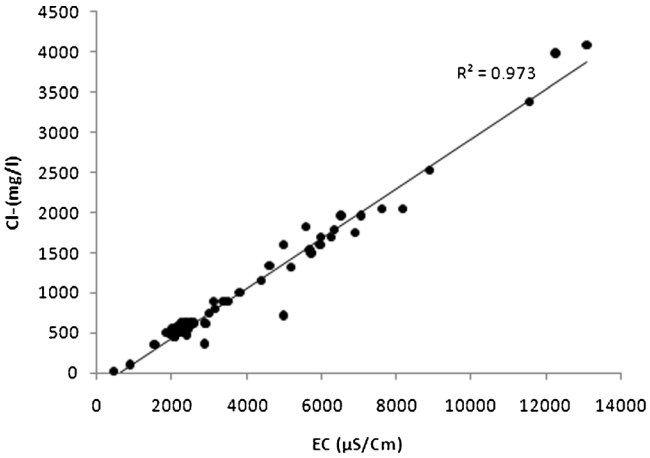

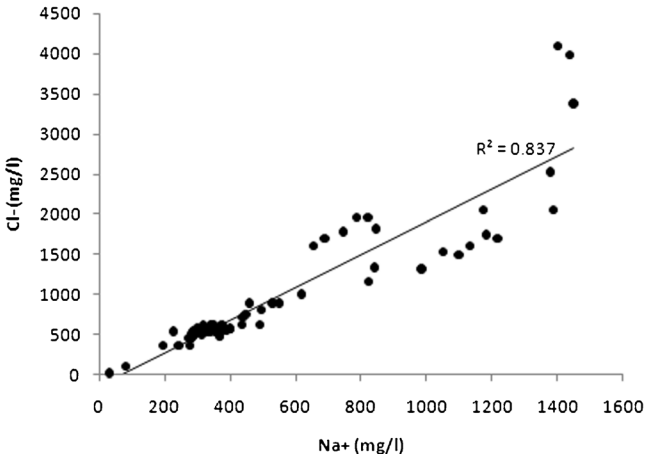

Fig. 4 Plots of: Na vs EC, Cl vs Ec and Cl vs Na

Table 4 Correlation coefficients of physicochemical parameters

	EC	Ca	Mg	Na	K	HCO_3	Cl	SO_4	NO_3
EC	1.00	0.88	0.84	0.93	0.76	0.68	0.98	0.63	0.80
Ca		1.00	0.82	0.72	0.61	0.51	0.90	0.38	0.82
Mg			1.00	0.67	0.50	0.42	0.87	0.50	0.69
Na				1.00	0.82	0.78	0.91	0.75	0.68
K					1.00	0.70	0.75	0.53	0.64
HCO_3						1.00	0.64	0.62	0.49
Cl							1.00	0.59	0.80
SO_4								1.00	0.47
NO_3									1.00

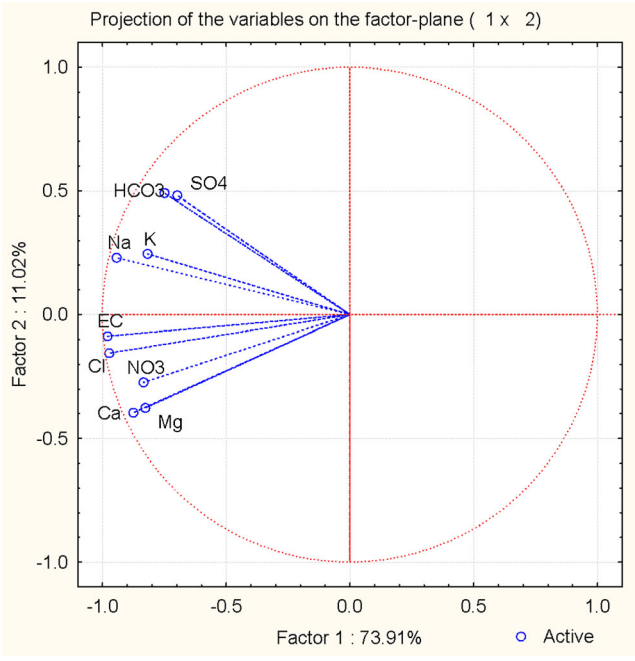

Fig. 5 Spatial distribution of the variables in the axes system F1–F2

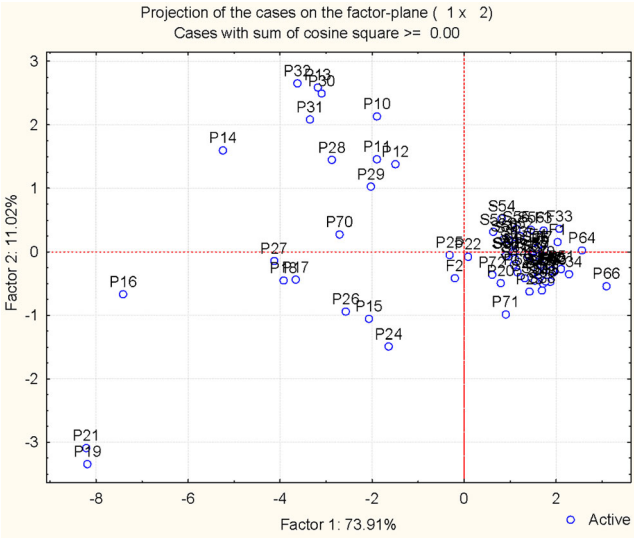

Fig. 6 Spatial distribution of the individuals in the axes system F1–F2

supersaturation of the groundwater with respect to that particular mineral phase, and that the water is incapable of dissolving more of the mineral (Kortatsi 2006). The calculated SI values for gypsum, anhydrite, and for most of the dolomite were less than zero (Table 3), indicating the undersaturation of groundwater in these minerals, which is in good agreement with the inferred dissolution of gypsum (Zhai et al. 2013). In contrast, the SI of calcite and aragonite ($CaCO_3$) indicated that the groundwater was supersaturated with these carbonate minerals, a fact corroborated by the presence of calcareous rocks.

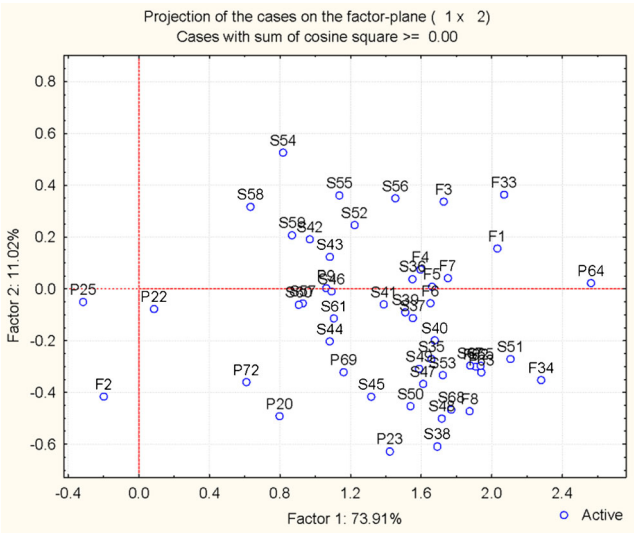

Fig. 7 Zoom of the spatial distribution of the individuals in the axes system F1–F2

The plots of Cl^- and Na^+ ions with EC show that the chloride and sodium were strongly correlated with EC with R^2= 0.973 and 0.868, respectively (Fig. 4). These indicate that groundwater salinities were mainly controlled by these ions. Thus, a plot of chloride versus sodium shows a high correlation coefficient of 0.837 (Fig. 4) indicating that these ions have the same origin, which can be (1) the dissolution of halite present in the sedimentary rocks and (2) the derivation from saline surface deposits.

PCA

The variables for PCA were EC, K^+, Na^+, Ca^{2+}, Mg^{2+}, HCO_3^-, Cl^-, SO_4^{2-}, and NO_3^- (Table 4). Two independent factors were extracted, which explained 84.93 % of the total variation (TV). The first one (F1) was responsible for 73.91 % of TV and was represented by EC, K^+, Na^+, Ca^{2+}, Mg^{2+}, Cl^-, and NO_3^-. The second factor (F2) explained 11.02 % of the TV and was mainly represented by HCO_3^- and SO_4^{2-}. The spatial distribution of the variables and individuals in the systems F1–F2 (Figs. 5, 6, and 7) shows the presence of three groups of waters. Group 1 corresponds to the waters of springs originating in the fault hosted by Upper Bajocian limestone formations. Group 2 corresponds to the waters of wells and boreholes situated in the irrigation zone, where agricultural activities take place (palm trees), hosted by quaternary alluvial formations in the south. Finally, group 3, in the north, characterizes the waters of wells located in Lower Bajocian and Liassic beds, consisting of alternating limestones, marls, and other carbonates.

^{18}O and ^{2}H stable isotopes

The isotopes ^{2}H and ^{18}O are excellent tracers, which can be used to determine the origin of groundwater and are widely used to study the circulation of natural water and groundwater movement (Vasanthavigar et al. 2013). The isotope compositions of well and spring waters that we obtained are plotted in Fig. 8. The WMWL is $\delta D=8\ \delta^{18}O+10‰$ (Craig 1961). The relationship between δD and $\delta^{18}O$ in groundwater samples suggests that the chemical composition was significantly modified by evaporation.

The $\delta^{18}O$ and δD values are in the range of −9.12 to −8.3 and −62.12 to −54.88‰, respectively. The $\delta^{18}O$ value decreases from north to south (high to low altitude). The linear correlation between $\delta^{18}O$ and δD of 1988 (Assou 1996) is similar to that of 2004. The regional altitude isotopic gradient of the Figuig oasis is estimated to be −0.9‰ per 100 m from samples collected in springs and wells, at different altitudes ranging from 856 to 941 m (Fig. 9). The low value of ^{18}O suggests that the paleo-recharge is of Holocene age.

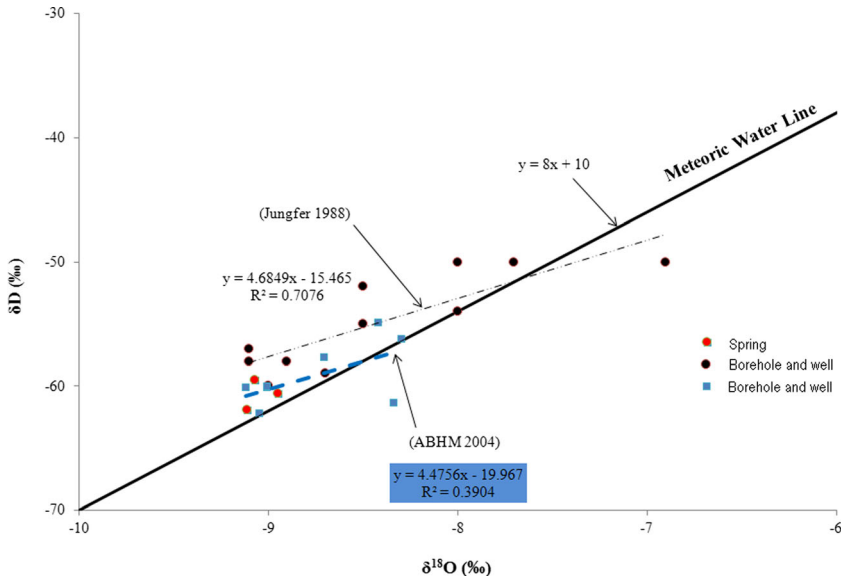

Fig. 8 $\delta^{18}O$-δD diagram of groundwater

^{13}C, ^{14}C, and ^{3}H geochemistry

The ^{13}C, ^{14}C, and ^{3}H values measured are in the ranges of −8.07 to −7.4‰, 22.31 to 33.76 pCm and 0.3 to 2.9 TU, respectively (Table 1). The different models used to estimate the age of groundwater (Eichinger 1983; Fontes and Garnier 1979; Ingerson and Pearson 1964) yield ages ranging between 2495 and 10,696 years (Holocene), see Table 5. These are in good agreement with the low values of ^{18}O and ^{3}H.

Conclusions

Water scarcity and degradation are significant problems in the Figuig oasis. Our research has identified two major types of groundwater chemistry: Na-Ca-Cl-HCO_3 and Na-Cl dominant. The EC of groundwater is low in the western and northern part of the study area and high in the southern part. We interpret the origin of salinity to be partly linked to the lithology of the geological formations and, to a lesser extent, to the

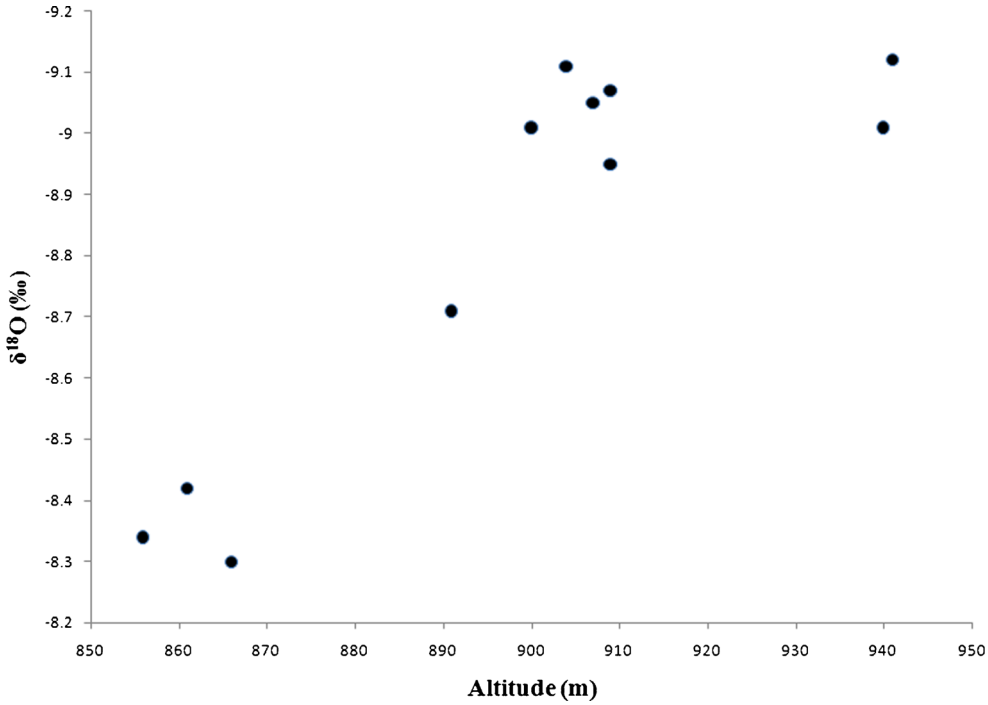

Fig. 9 Altitude isotopic gradient of the Figuig oasis

Table 5 Mean residence time of the water based on different models

Model	Name			
	F62	F63	P66	P71
Age (Ingerson and Pearson 1964)	7906	7664	3748	4400
Age (Eichinger 1983)	6444	6715	2495	3442
Age (Fontes and Garnier 1979)	9817	10,696	6943	8730

irrigation/evaporation processes in the palm groves. Multivariate statistical analysis carried out using PCA of major hydrochemical ions has identified two major geochemical processes with 84.93 % of TV. The relationship of ^{2}H and ^{18}O shows that the initial isotopic composition has been modified by the evaporation processes during local water infiltration. Finally, we have been able to constrain the age of the groundwater as ranging from 2495 to 10,696 years. Our findings are important, as they provide the basis for a much better understanding and, therefore, much better management of the vital water resources of the Figuig aquifer.

Acknowledgments The author wishes to thank the journal reviewers and Dr. Mike Mlynarczyk for helping improve this manuscript.

References

Abderamane H, Razack M, Vassolo S (2013) Hydrogeochemical and isotopic characterization of the groundwater in the Chari-Baguirmi depression, Republic of Chad. Environ Earth Sci 69(7):2337–2350

Assou M (1996) Salinité des sols et qualité des eaux d'irrigation de l'oasis de Figuig. Ministère de l'agriculture et de la mise en valeur agricole, Administration du génie rural, Direction du développement et de la gestion de l'irrigation. Rabat, 99 p.

Craig H (1961) Isotopic variations in meteoric water. Sci 133:1702–1703

Eichinger L (1983) A contibution to the interpretation of 14C groundwater ages considering the exemple of a partially confined sandstone aquifer. Radiocarbon 25(2):347–356

Fontes J-C, Garnier J-M (1979) Determination of the initial 14C activity of the total dissolved carbon: a review of the existing models and a new approach. Water Resour Res 15(2):399–413

Ingerson E, Pearson F-J (1964) Estimation of age and rate of motion of groudwater by the 14C method. In: Recent Researches in the Fields of Hydrosphere, Atmosphere and Nuclear Geochemistry (ed. by Maruzen). Maruzen, Tokyo, Japan, pp 263–283

Jilali A (2014a) Contribution à la compréhension du fonctionnement hydrodynamique de la nappe souterraine de l'oasis de Figuig (Haut Atlas Oriental). Université Mohammed Premier, Oujda, 161 pp

Jilali A (2014b) Impact of climate change on the Figuig aquifer using a numerical model: oasis of Eastern Morocco. J Biol Earth Sci 4(1): E16–E24

Jilali A, Zarhloule Y (2015) Structural control of the hydrogeology in Figuig Oasis in the eastern High Atlas of Morocco. P Geologists Assoc 126(2):232–243

Jilali A, Abbas M, Amar M, Zarhloule Y (2015a) Groundwater contamination by wastewater in Figuig Oasis (eastern High Atlas, Morocco). Nature Environ Pollu Techno 14(2):275–282

Jilali A, Amar M, Zarhloule Y, Amar N, Kerchaoui S, Baba E (2015b) Apport de la géophysique à la compréhension des structures géologiques de l'oasis de Figuig (Haut Atlas Oriental, Maroc). J Materials Environ Sci 6(1):236–245

Jilali A, Zarhloule Y, Georgiadis M (2015c) Vulnerability mapping and risk of groundwater of the oasis of Figuig, Morocco: application of DRASTIC and AVI methods. Arab J Geosci 8(3):1611–1621

Kortatsi B (2006) Hydrochemical characterization of groundwater in the Accra plains of Ghana. Environ Geol 50(3):299–311

Kumar M, Herbert J-R, Ramanathan A-L, Someshwar Rao M, Kim K, Deka J-P, Kumar B (2013) Hydrogeochemical zonation for groundwater management in the area with diversified geological and land-use setup. Chem Erde-Geochem 73(3):267–274

Parkhurst D-L, Appelo C-A-J (1999) User's guide to PHREEQC (Version 2): a computer program for speciation, batch-reaction, one-dimensional transport, and inverse geochemical calculations. Water-Resources Investigations Report. USGS, Denver, Colorado, 99–4259, p 312

Rodier J (1984) L'analyse de l'eau: eaux naturelles, eaux résiduaires, eau de mer. Dunod, 7th ed, Paris

Thivya C, Chidambaram S, Thilagavathi R, Prasanna M-V, Singaraja C, Nepolian M, Sundararajan M (2013) Identification of the geochemical processes in groundwater by factor analysis in hard rock aquifers of Madurai District. South India Arab J Geosci 1–11

Tlili-Zrelli B, Hamzaoui-Azaza F, Gueddari M, Bouhlila R (2013) Geochemistry and quality assessment of groundwater using graphical and multivariate statistical methods. A case study: Grombalia phreatic aquifer (Northeastern Tunisia). Arab J Geosci 6(9):3545–3561

Vasanthavigar M, Srinivasamoorthy K, Prasanna M-V (2013) Identification of groundwater contamination zones and its sources by using multivariate statistical approach in Thirumanimuthar sub-basin, Tamil Nadu, India. Environ Earth Sci 68(6):1783–1795

Wang P, Yu J, Zhang Y, Liu C (2013) Groundwater recharge and hydrogeochemical evolution in the Ejina Basin, northwest China. J Hydrol 476:72–86

Wildemeersch S, Orban P, Ruthy I, Grière O, Olive P, El Youbi A, Dassargues A (2010) Towards a better understanding of the Oulmes hydrogeological system (Mid-Atlas, Morocco). Environ Earth Sci 60(8):1753–1769

Wu J, Li P, Qian H, Duan Z, Zhang X (2013) Using correlation and multivariate statistical analysis to identify hydrogeochemical processes affecting the major ion chemistry of waters: a case study in Laoheba phosphorite mine in Sichuan. China Arab J Geosci 1–10

Zhai Y, Wang J, Teng Y, Zuo R (2013) Hydrogeochemical and isotopic evidence of groundwater evolution and recharge in aquifers in Beijing Plain, China. Environ Earth Sci 69(7):2167–2177